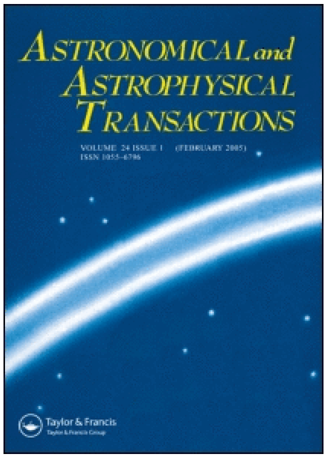

Astronomical & Astrophysical Transactions
The Journal of the Eurasian Astronomical Society
Publication details, including instructions for authors and subscription information:
http://www.informaworld.com/smpp/title~content=t713453505

Magnetic field decay in neutron star cores

V. A. Urpin [a]; D. A. Shalybkov [a]
[a] A. F. Ioffe Institute of Physics and Technology, St. Petersburg, Russia

Online Publication Date: 01 March 1994
To cite this Article: Urpin, V. A. and Shalybkov, D. A. (1994) 'Magnetic field decay in neutron star cores', Astronomical & Astrophysical Transactions, 4:4, 251 - 259
To link to this article: DOI: 10.1080/10556799408205381
URL: http://dx.doi.org/10.1080/10556799408205381

Astronomical and Astrophysical Transactions, 1994,
Vol. 4, pp. 251–259

MAGNETIC FIELD DECAY IN NEUTRON STAR CORES

V. A. URPIN and D. A. SHALYBKOV

A. F. Ioffe Institute of Physics and Technology 194021, St. Petersburg, Russia

(Received 17 July, 1992)

Electric resistivity of a neutron star interior can be enhanced by magnetic field producing dramatic enhancement of the ohmic dissipation. The diffusion and dissipation of an axisymmetric toroidal magnetic field in a neutron star core is considered. It is shown that the ohmic decay time may be as short as $\sim 10^6$ years. The dissipation may noticeably heat the core and delay the cooling of a star of age $\gtrsim 10^6$ years.

KEY WORDS Neutron stars, magnetic field decay, cooling

1. INTRODUCTION

Many neutron stars possess strong magnetic fields $B \sim 10^{12}$–10^{13} G. These fields are important for a variety of phenomena inside the neutron stars and in their vicinities. There is no generally accepted point of view on the origin and evolution of neutron star magnetic fields. It is possible that the fields are confined in the surface stellar layers. For instance, the thermomagnetic effects can generate magnetic fields during early stages of the neutron star evolution (see, Blandford *et al.*, 1983; Urpin *et al.*, 1986). However one cannot exclude that strong fields are inherited from neutron star progenitors and amplified when the progenitors collapse into neutron stars. Magnetic flux conservation during the collapse phase can produce the fields $\sim 10^{13}$ G if the progenitor fields are $\sim 10^3$ G.

Since the nature of magnetic fields is unknown one can analyze various assumptions. Comparing theoretical results with observational data, one can obtain important information about the magnetic field location and about the field decay mechanisms. In the present paper we assume that the magnetic field occupies initially a significant fraction of the neutron star core. The core will be thought to be composed of normal *npe*-matter (without superfluidity and superconductivity). It has been widely recognized after the classical work of Baym *et al.* (1969) that the decay time of interior magnetic fields is larger than the Universe age. Recently Haensel *et al.* (1991) have reconsidered the problem. They have shown (see also Yakovlev and Shalybkov, 1991) that magnetic fields can strongly magnetize motion of charged particles in neutron star cores. This drastically decreases the conductivity $\sigma_\perp$ across $\vec{B}$ and the ohmic decay time of the internal magnetic fields. According to a qualitative analysis of Haensel *et al.* (1991), a typical time scale of magnetic field dissipation can be $\sim 10^7$ yrs. Note that this mechanism enhances the decay of electrical currents transverse to $\vec{B}$.

Longitudinal currents decay essentially slower since the longitudinal conductivity is not affected by $\vec{B}$. However, the strong dissipation mechanism proposed by Haensel *et al.* (1991) can produce rapid decay of various magnetic configurations. For instance, the decay of any toroidal magnetic field is determined by $\sigma_\perp$ because a toroidal field is supported by transverse currents. The same is true for a dipolar magnetic configuration.

In this paper we will consider the evolution of a toroidal magnetic configuration. The statement of the problem is the simplest mathematically for this configuration. Besides, the solution for the toroidal field yields a reliable estimate for the decay time scales of other magnetic configurations where magnetic fields and currents are perpendicular. Note also that if the neutron star core contains a magnetic field, its toroidal component is most likely larger than the poloidal one. This is because the newly born neutron star should spin nonrigidly even if the progenitor possessed rigid rotation. Since the conductivity is high, the magnetic field will be "frozen" into the plasma due to typically large magnetic Reynolds number, $\mathrm{Re}_m \sim \sigma R^2 \Delta\Omega / c^2 \gg 1$, where $\Delta\Omega$ is the deviation of the angular velocity from the rigid rotation and R is the stellar radius. Differential rotation generates a strong toroidal magnetic field from the poloidal one. The generation time scale is very short, $\sim 1/\Delta\Omega$. The field generation will probably be stopped by nonlinear magnetohydrodynamical effects. The quasistationary toroidal field produced by this mechanism should be much higher than the original poloidal field.

The paper is organized as follows. In Sec. 2 the electrical conductivity of matter in neutron star cores is briefly considered. In Sec. 3 the main equations are presented that govern the field decay and Joule reheating of neutron star cores. Sec. 4 presents the results of computations. The results are discussed briefly in Sec. 5.

2. *Conductivity of matter in neutron star cores*

We assume that matter of neutron star cores consists of free strongly degenerate electrons, protons and neutrons in normal state. In the presence of a magnetic field $\vec{B}$ the electrical conductivity and resistivity are anisotropic. They are described by the tensors $\hat{\sigma}$ and $\hat{\mathscr{R}}$, respectively. If the axis z is parallel to $\vec{B}$, these tensors read

$$\hat{\sigma} = \begin{pmatrix} \sigma_\perp & \sigma_\wedge & 0 \\ -\sigma_\wedge & \sigma_\perp & 0 \\ 0 & 0 & \sigma_\parallel \end{pmatrix}, \qquad \hat{\mathscr{R}} = \begin{pmatrix} \mathscr{R}_\perp & \mathscr{R}_\wedge & 0 \\ -\mathscr{R}_\wedge & \mathscr{R}_\perp & 0 \\ 0 & 0 & \mathscr{R}_\parallel \end{pmatrix}. \tag{1}$$

Here $\sigma_\parallel$ and $\mathscr{R}_\parallel$ are, respectively, the longitudinal conductivity and resistivity; $\sigma_\perp$ and $\mathscr{R}_\perp$ denote the transverse conductivity and resistivity components, while $\sigma_\wedge$ and $\mathscr{R}_\wedge$ are the Hall components. The magnetic fields in neutron star interiors are commonly non-quantizing, and one has $\mathscr{R}_\parallel = \sigma_\parallel^{-1} = \mathscr{R}_0$, where $\mathscr{R}_0$ is the resistivity at $B = 0$. The anisotropic character of $\hat{\sigma}$ and $\hat{\mathscr{R}}$ is described by two parameters, α_e and α_p,

$$\alpha_e = \frac{eB\tau_e}{m_e^* c} = 7.2 \frac{B_{12}}{T_9^2} \frac{\rho}{\rho_0}, \qquad \alpha_p = \frac{eB\tau_p}{m_p^* c} = 2 \cdot 10^{-3} \frac{B_{12}}{T_9^2} \left(\frac{\rho}{\rho_0}\right)^{1/3}, \tag{2}$$

where τ_e and τ_p are the relaxation times for electrons and protons, respectively,

m_p^* is the effective proton mass; $B_{12}=B/10^{12}G$, $T_9=T/10^9\,\mathrm{K}$, and $\rho_0=2.8\cdot10^{14}\,\mathrm{g/cm^3}$ is the standard nuclear density. The electron relaxation time is determined by the Coulomb scattering on protons, and the proton relaxation time by nuclear interactions with neutrons. For normal *npe*-matter, one has (see, e.g., Yakovlev and Shalybkov, 1991)

$$\mathcal{R}_\perp=\mathcal{R}_0(1+\alpha_0^2),\qquad \mathcal{R}_\wedge=\mathcal{R}_0\alpha_e,\qquad \alpha_0=(\alpha_e\alpha_p)^{1/2}\approx0.12\frac{B_{12}}{T_9^2}\left(\frac{\rho}{\rho_0}\right)^{2/3}, \tag{3}$$

$$R_0\approx6.06\cdot10^{-27}\left(\frac{\rho_0}{\rho}\right)^3T_9^2\left(1+\frac{\rho}{2\rho_0}\right)s.$$

If $\alpha_0<1$, then $\mathcal{R}_\perp\simeq\mathcal{R}_0$ and the effect of the magnetic field on the ohmic decay is insignificant. If $\alpha_0>1$, the resistivity across the field strongly increases and accelerates the ohmic decay. In this case $\mathcal{R}_\perp\propto T^{-2}$, so that the neutron star cooling amplifies the field decay. If the electric current is transverse to $\vec{B}$, the importance of the Hall drift can be characterized by the parameter $\alpha=R_\wedge/R_\perp=\alpha_e/(1+\alpha_0^2)$. If $\alpha_e<1$ (and, hence, $\alpha_p<1$), the Hall drift is negligible. If $\alpha_e>1$ and $\alpha_p<1$, the Hall effect can be important, but cannot essentially change the field decay rate. For strong fields, which magnetize the protons ($\alpha_p>1$), α is small again and the Hall drift is unimportant. The maximum value $\alpha_m\approx42(\rho_0/\rho)$ is reached at $\alpha_0=1$.

It is qualitatively clear that the B^2 dependence of $\mathcal{R}_\perp$ should lead to a more uniform field distribution within the neutron star core: the dissipation rate is proportional to $\mathcal{R}_\perp\propto B^2$ and higher fields decay faster.

3. *The statement of the problem*

For simplicity, consider ohmic decay in a neutron star core with uniform density. Excluding the very early evolution stage, the core can be assumed to be isothermal because the main temperature gradients occur in the surface layers (see, e.g., Gudmundsson *et al.* 1983, Van Riper 1991).

In the absence of hydrodynamical flows the magnetic field obeys the induction equation

$$\frac{\partial\vec{B}}{\partial t}=-\frac{c^2}{4\pi}\nabla\times[\hat{\mathcal{R}}(\nabla\times\vec{B})]. \tag{4}$$

Consider the decay of a toroidal magnetic configuration that has the φ-component alone: $\vec{B}=B(r,\theta,t)\vec{e}_\varphi$, where r, θ, φ are polar coordinates and $\vec{e}_\varphi$ is the azimuthal unit vector. From Equation (4) one obtains

$$\frac{\partial B}{\partial t}=\frac{c^2}{4\pi r}\left\{\frac{\partial}{\partial r}\left[\mathcal{R}_\perp\frac{\partial}{\partial r}(rB)\right]+\frac{1}{r}\frac{\partial}{\partial\theta}\left[\frac{\mathcal{R}_\perp}{\sin\theta}\frac{\partial}{\partial\theta}(B\cdot\sin\theta)\right]\right.$$
$$\left.+\cot\theta\frac{\partial}{\partial r}(\mathcal{R}_\wedge B)+\frac{\partial B}{\partial\theta}\frac{\partial\mathcal{R}_\wedge}{\partial r}-\frac{\partial B}{\partial r}\frac{\partial\mathcal{R}_\wedge}{\partial\theta}-\frac{1}{r}\frac{\partial}{\partial\theta}(\mathcal{R}_\wedge B)\right\}. \tag{5}$$

$B(r,\theta,t)$ should obey the standard boundary conditions for the toroidal field

$$B=0\quad\text{at}\quad r=0\quad\text{and}\quad r=R, \tag{6}$$

where R is the stellar radius. The initial field distribution has been taken in the form

$$B|_{t=0} = B_0 \sin\theta\left[\frac{\sin(kr)}{(kr)^2} - \frac{\cos(kr)}{kr}\right], \qquad k = 4.493/R. \tag{7}$$

Here B_0 determines the amplitude of the initial field. Equation (7) describes the fundamental toroidal field mode for the case of $\mathcal{R}_\perp = \text{const}$ and $\mathcal{R}_\wedge = 0$.

As follows from Eq. (3), $\mathcal{R}_\perp$ and $\mathcal{R}_\wedge$ depend on temperature. Therefore, to complete the equations, one should add the equation of thermal balance. For the isothermal and uniform core, this equation can be written as

$$C_v V \frac{\mathrm{d}T_c}{\mathrm{d}t} = -V\varepsilon_v - L_{\mathrm{ph}}(T_e) - \frac{1}{4\pi}\int B\frac{\partial B}{\partial t}\,\mathrm{d}v. \tag{8}$$

Here C_v is the specific heat of matter in the neutron star core, ε_v is the neutrino emissivity (per unit volume), $L_{\mathrm{ph}}(T_e) = 4\pi\Sigma R^2 T_e^4$ is the photon luminosity of the star; Σ is the Stefan–Boltzmann constant; $V = 4\pi R^3/3$. The third term on the right-hand side of (8) describes the reheating of matter due to ohmic dissipation. The initial temperature has been set equal to 10^9 K. In fact, the field decay is almost independent of the initial temperature. During the early evolution stage the star cools to $\sim 10^8$ K very rapidly due to neutrino emission. The field decay time is longer than the duration of this stage. Therefore one can take any initial temperature $\gtrsim 10^8$ K. In our case the heat content is mainly determined by degenerate neutrons (Maxwell, 1979),

$$C \approx 1.64 \cdot 10^{20}\left(\frac{\rho}{\rho_0}\right)^{1/3} T_9 \frac{\mathrm{erg}}{\mathrm{cm^3\,K}}. \tag{9}$$

The main contribution to the neutrino emissivity comes from the modified URCA-processes,

$$\varepsilon_v \approx 2.7 \cdot 10^{21}\left(\frac{\rho}{\rho_0}\right)^{2/3} T_9^8 \frac{\mathrm{erg}}{\mathrm{cm^3\,K}}. \tag{10}$$

The photon luminosity L_{ph} depends on the surface temperature T_e. Hence, one should know the relationship between T_e and the central temperature T_c. We have used the relationship obtained by Gudmundsson *et al.* (1983),

$$T_{c9} = 0.1288(T_{e6}^4/g_{14})^{0.455}, \tag{11}$$

where $T_{c9} = T_c/10^9$ K, $T_{e6} = T_e/10^6$ K, $g_{14} = g/10^{14}$ cm/s^2, $g = GMR^{-2}(1 - 2GM/Rc^2)^{-1/2}$ is the surface gravity, and M is the neutron star mass. Note that Eq. (11) has been obtained for a star whose surface magnetic fields are not too high to affect the $T_c(T_e)$ dependence. Equation (11) is strictly valid for $10^5\ \mathrm{K} \le T_e \le 10^{6.5}$ K and gives an order-of-magnitude estimate at lower T_e.

4. *Numerical results*

Equations (5) and (8) have been solved numerically with the above boundary and initial conditions. Computations have been performed for neutron star models

Table 1

Model	*Radius*	*Density, g/cm*^{3}
1	$7.34 \cdot 10^6$	$1.9 \cdot 10^{15}$
2	$10.6 \cdot 10^6$	$5.6 \cdot 10^{14}$
3	$15.8 \cdot 10^6$	$1.7 \cdot 10^{14}$

with $M = 1.4\,M_\odot$ and three different values of R, corresponding to different equations of state of nuclear matter. The values of R are listed in Table 1. The initial field amplitude B_0 in Eq. (7) has been varied from 10^{13} to 10^{15} G. The initial magnetic field (7) reaches maximum $B_m \approx 0.436\ B_0$ at $r \approx 0.463\ R$ in the equatorial plane.

Figure 1 shows evolution of magnetic configuration for Model 2 and $B_0 = 10^{13}$ G. The field distribution becomes more uniform with time (as explained in Sect. 2). The dissipation produces the drift of the regions of maximum electric current (i.e., of maximum non-uniformity of B) either to the surface or to the symmetry axis. Accordingly, the currents are pushed out of the core during the evolution. This seems to be quite natural because the currents have longer decay time scales in regions with higher conductivity. In our case the highly conducting regions lie near the surface and polar axis, where $B = 0$.

Figure 2 shows the field decay for Model 2 and $B_0 = 10^{13}$, 10^{14} and 10^{15} G. The field dissipates effectively due to the increase of the transverse resistivity. At the initial stage ($t \lesssim 2 \cdot 10^6$ yrs) the e-folding ohmic decay time is $4 \cdot 10^5$, 10^6 and $2 \cdot 10^6$ yrs for $B_0 = 10^{15}$, 10^{14} and 10^{13} G, respectively. At $t \gtrsim 2 \cdot 10^6$ yrs the typical decay time scale is $\sim 10^6$ yrs for all the configurations of study. The maximum field strengths $B_m(t)$ for different B_0 become closer with time. In particular, at $t = 8 \cdot 10^6$ yrs, B_m for $B_0 = 10^{15}$ G is only a factor of ~ 4 larger than for $B_0 = 10^{13}$ G. The ohmic decay in the core is so efficient that $B_m(t) < 10^{11}$ G at $t \sim 10^7$ yrs for any B_0. The field decay is essentially non-exponential. The curves

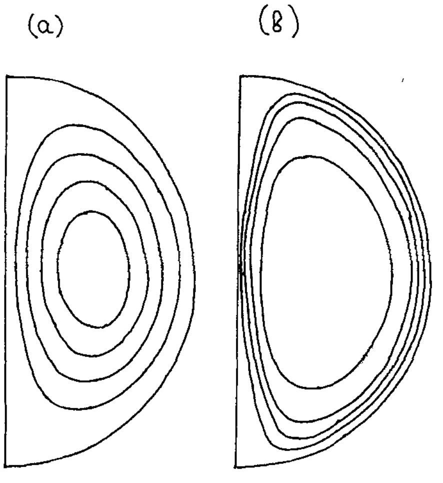

Figure 1 Contours of constant toroidal magnetic field for Model 2 with $B_0 = 10^{13}$ G for (a) $t = 0$, and (b) $t = 7.6 \cdot 10^6$ yrs.

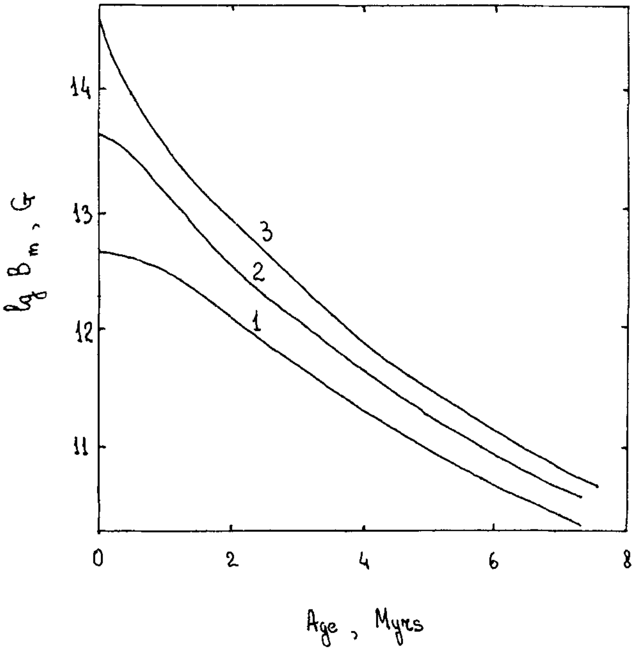

Figure 2 Maximum field strength B_m versus age for Model 2 at $B_0 = 10^{13}$ G (curve 1), 10^{14} G (curve 2), 10^{15} (curve 3).

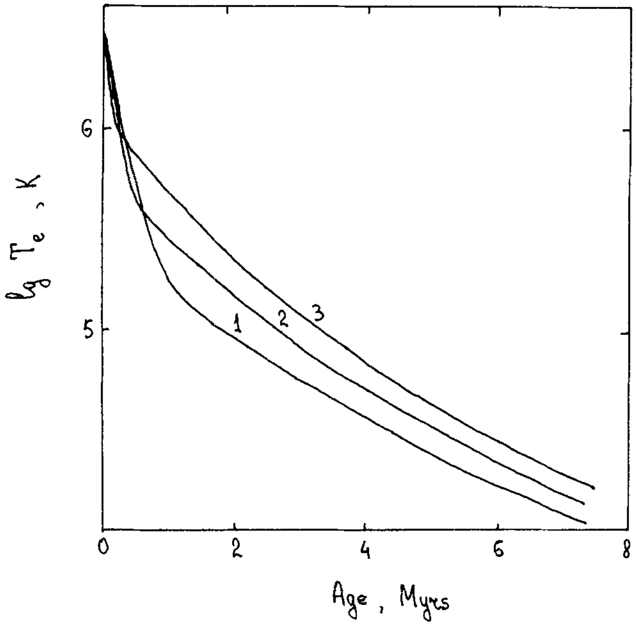

Figure 3 Surface temperature T_e versus age for Model 2 at $B_0 = 10^{13}$ G (curve 1), 10^{14} G (curve 2) and 10^{15} G (curve 3).

in Figure 2 can be fitted by the expressions

$$B_m(t) = 0.463B_0 \begin{cases} \exp[-t^{1.88}(2.2 \cdot 10^{11} + 5.8 \cdot 10^7 t^{1.07})^{-1}], & \text{for} \quad B_0 = 10^{13}\,\mathrm{G} \\ \exp[-5.0 \cdot 10^{-5} t^{0.75}], & \text{for} \quad B_0 = 10^{14}\,\mathrm{G} \\ \exp[-5.0 \cdot 10^{-4} t^{0.62}], & \text{for} \quad B_0 = 10^{15}\,\mathrm{G} \end{cases} \tag{12}$$

where t is age in yrs. The fitting errors of (12) are not larger than few percent.

Figure 3 shows the cooling curves for Model 2 at $B_0 = 10^{13}$, 10^{14} and 10^{15} G. If $B_0 \lesssim 10^{13}$, the Joule reheating is negligible. On the contrary, the ohmic dissipation can essentially slow the neutron star cooling for higher B_0. The reheating is especially important at late evolutionary stages ($t \gtrsim 10^5$ yrs for $B_0 = 10^{15}$ G, and $t \gtrsim 10^6$ yrs for $B_0 = 10^{14}$ G). At these stages the ohmic reheating can increase the neutron star luminosity by a factor of ~10–100.

Figure 4 shows the dependence of the magnetization parameter α_0 for Model 2 at $B_0 = 10^{13}$, 10^{14} and 10^{15} G. In the course of the evolution α_0 increases monotonically with time and reaches very large values. This is because the field decay is slower than the cooling, i.e. the magnetization parameter, which is proportional to B/T_c^2, increases. The effect is especially strong at early evolutionary stage when cooling is determined by the neutrino emissivity. The growth of α_0 accelerates the field decay. However, the enhanced decay produces more uniform magnetic configurations which dissipate slower. Owing to the competition of these processes, which act in opposite directions, the ohmic decay becomes slower with time.

Figure 5 displays evolution of the maximum field for $B_0 = 10^{13}$ G and different

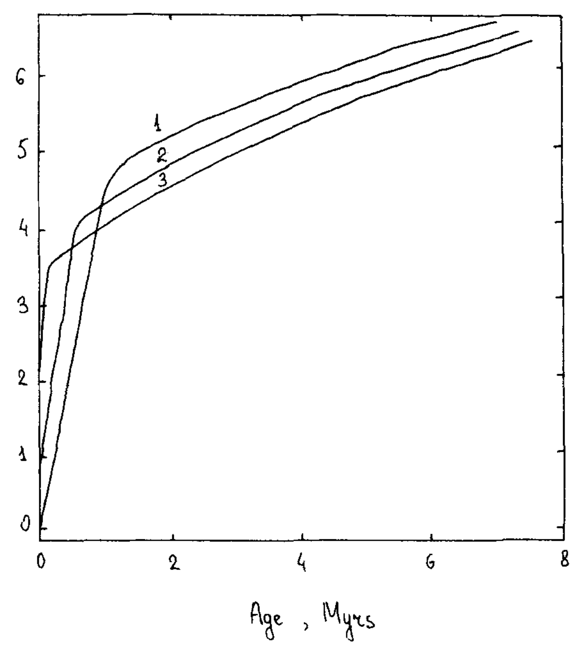

Figure 4 Magnetization parameter α_0 versus age for Model 2 at $B_0 = 10^{13}$ G (curve 1), 10^{14} G (curve 2), and 10^{15} G (curve 3).

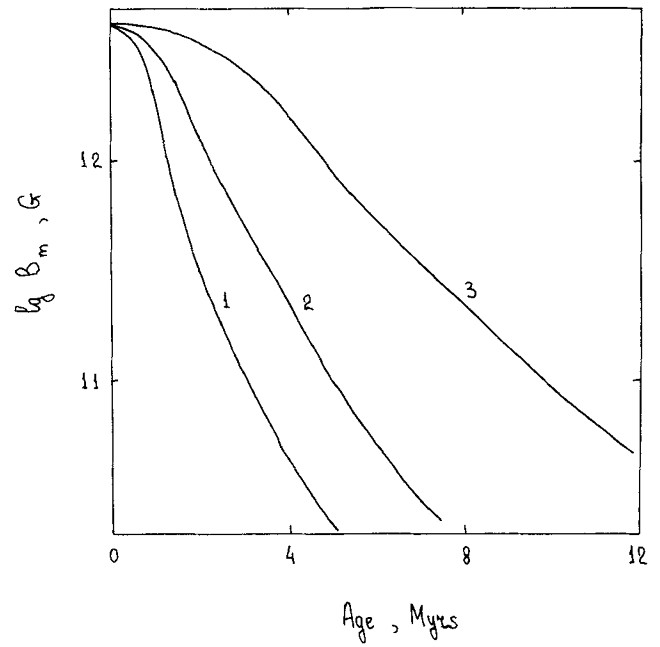

Figure 5 Maximum field strength B_m versus age for different neutron star models at $B_0 = 10^{13}$ G. Numbers label models (see Table).

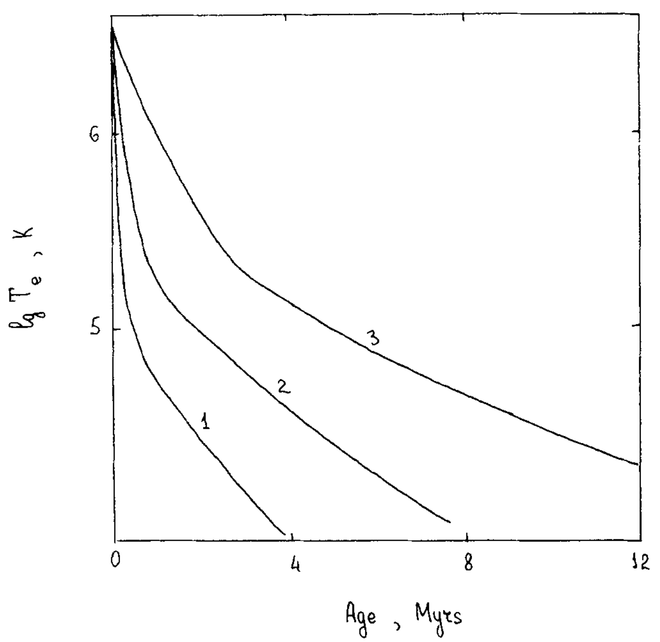

Figure 6 Surface temperature T_e versus age for Models 1, 2 and 3.

stellar models. The field decay is sensitive to the stellar models. The fastest decay occurs for Model 1 which has the smallest radius. The slowest decay takes place for Model 3. The decay time scales at the early evolutionary stage are 10^6, $2 \cdot 10^6$ and $4 \cdot 10^6$ yrs for Models 1, 2 and 3, respectively. The difference comes mainly from the different electric conductivities, which depend on the density of matter in the core.

Figure 6 displays cooling curves for different models with $B_0 = 10^{13}$ G. The behaviour of the curves is sensitive to stellar models. The difference is especially large at late evolutionary stages when the ohmic dissipation becomes important in the thermal balance. Model 1, in which the field decay goes faster, shows faster cooling. Model 3 with slower decaying field shows slower cooling.

5. *Conclusions*

In this paper we have considered the field decay in a neutron star whose core consists of a normal *npe*-matter. Strong magnetic fields can magnetize motion of charge particles and enhance the transverse resistivity producing rapid decay of electric currents perpendicular to $\vec{B}$. For magnetic configurations with currents transverse to $\vec{B}$, this yields a rapid field dissipation. If the field geometry is more complicated, then the rapid dissipation of $\vec{j}_\perp$ will probably produce a field-free configuration.

According to our results the field decay due to the enhancement of $\mathcal{R}_\perp$ can be very efficient. If $B_0 \geq 10^{13}$ G, the decay time scale may be of the order of 10^7 yrs. The maximum field strengths for configurations with different initial magnetic fields become closer with time. The field decay depends on the equation of state in the neutron star core: the equation of state determines the density in the core and, hence, the conductivity. The magnetic field dissipation and associated ohmic reheating can lead to a considerable delay of the neutron star cooling.

Note also that the behaviour of the magnetic fields in the surface layers of neutron stars may be quite different from the behaviour of the internal fields due to much slower field diffusion in the crust (see Urpin, this volume).

This work was supported by a grant of American Astronomical Society.

References

Baym, G., Pethick, C. and Pines, D. (1969). Electrical conductivity of neutron star matter. *Nature*. **224**, 673–674.

Blandford, R., Applegate, J. and Hernquist, L. (1983). Thermal origin of neutron star magnetic fields. *Mon. Not. R. astr. Soc.* **204**, 1025–1048.

Gudmundsson, E., Pethick, C. J. and Epstein, R. I. (1983). Neutron star envelopes. *Astrophys. J.* **272**, 286–290.

Haensel, P., Urpin, V. A. and Yakovlev, D. G. (1991) Ohmic decay of internal magnetic fields in neutron stars. *Astron. Astrophys.* **229**, 133–139.

Urpin, V. A., Levshakov, S. A. and Yakovlev, D. G. (1986) Generation of neutron star magnetic field by thermomagnetic effects. *Mon. Not. R. Astr. Soc.* **219**, 703–717.

Van Riper, K. A. (1991) Neutron star thermal evolution. *Astrophys. J. Suppl.* **75**, 449–462.

Yakovlev, D. G. and Shalybkov, D. A. (1991) Electrical conductivity of the neutron star interiors. *Astrophys. Space Sci.* **176**, 171–190.